

Dynamical onset of superconductivity and retention of magnetic fields in cooling neutron stars

Wynn C. G. Ho,^{1,2,*} Nils Andersson,¹ and Vanessa Graber³

¹*Mathematical Sciences and STAG Research Centre, University of Southampton, Southampton SO17 1BJ, United Kingdom*

²*Physics and Astronomy, University of Southampton, Southampton SO17 1BJ, United Kingdom*

³*Department of Physics and McGill Space Institute, McGill University, Montreal, Quebec, H3A 2T8, Canada*

(Received 12 July 2017; revised manuscript received 25 August 2017; published 4 December 2017)

A superconductor of paired protons is thought to form in the core of neutron stars soon after their birth. Minimum energy conditions suggest magnetic flux is expelled from the superconducting region due to the Meissner effect, such that the neutron star core is largely devoid of magnetic fields for some nuclear equation of state and proton pairing models. We show via neutron star cooling simulations that the superconducting region expands faster than flux is expected to be expelled because cooling timescales are much shorter than timescales of magnetic field diffusion. Thus magnetic fields remain in the bulk of the neutron star core for at least 10^6 – 10^7 yr. We estimate the size of flux free regions at 10^7 yr to be $\lesssim 100$ m for a magnetic field of 10^{11} G and possibly smaller for stronger field strengths. For proton pairing models that are narrow, magnetic flux may be completely expelled from a thin shell of approximately the above size after 10^5 yr. This shell may insulate lower conductivity outer layers, where magnetic fields can diffuse and decay faster, from fields maintained in the highly conducting deep core.

DOI: 10.1103/PhysRevC.96.065801

I. INTRODUCTION

Neutron stars (NSs) are unique probes of the dense matter equation of state (EOS), which prescribes a relationship between pressure and density and determines the behavior of matter near and above nuclear densities ($n_{\text{nuc}} \approx 0.16 \text{ fm}^{-3}$). For example, some EOSs predict the presence of exotic particles, such as hyperons and deconfined quarks, in the NS inner core at baryon number densities $n_b > n_{\text{nuc}}$ (see, e.g., [1,2], for review). At the same time, theory and observations indicate that the core of NSs (at $n_b \gtrsim 0.1 \text{ fm}^{-3}$) may contain a neutron superfluid and proton superconductor [3–6].

In this present work, we are concerned with the onset of proton superconductivity, which takes place when the local temperature T falls below the proton critical temperature T_{cp} (see, e.g., [7,8], for review). The latter is related to the energy gap for Cooper pairing Δ in the zero temperature limit by $k_B T_{\text{cp}} \approx 0.5669\Delta$ for singlet (1S_0) pairing. A paired proton superconductor can take two forms in the core of a NS, depending on the Ginzburg-Landau parameter

$$\kappa \equiv \lambda/\xi \quad (1)$$

and two critical magnetic fields

$$H_{c1} = \frac{\phi_0}{4\pi\lambda^2} \ln \kappa \quad \text{and} \quad H_{c2} = \frac{\phi_0}{2\pi\xi^2}, \quad (2)$$

where $\phi_0 = \pi\hbar c/e$ is the magnetic flux quantum and the equation for H_{c1} is in the limit of large κ [9]. The magnetic field penetration length scale is

$$\lambda = \left(\frac{m_p^* c^2}{4\pi e^2 n_e} \right)^{1/2} \quad (3)$$

and the superconductor pairing or coherence length scale (also typical size of magnetic fluxtube) is

$$\xi = \frac{2\varepsilon_F}{\pi k_F \Delta} = \frac{\hbar^2 k_F}{\pi m_p^* \Delta}, \quad (4)$$

where m_p^* is effective proton mass, ε_F and $\hbar k_F = \hbar(3\pi^2 n_p)^{1/3}$ are Fermi energy and momentum, respectively, and n_e and n_p are electron and proton number densities, respectively.

If the Ginzburg-Landau parameter $\kappa < 1/\sqrt{2}$, then an external magnetic field H does not penetrate significantly into the superconductor, and magnetic flux is expelled from superconducting regions (such that $B = 0$) due to the Meissner effect (see, e.g., [7,9–11]). In this state, magnetic flux can be retained in macroscopic regions of normal conducting matter that alternate with regions of flux-free superconducting matter. Conversely, if $\kappa > 1/\sqrt{2}$, then magnetic field can reside in superconducting fluxtubes. Substituting Eqs. (3) and (4) into Eq. (1), we find

$$\kappa \approx 0.8(\Delta/1 \text{ MeV})(n_p/n_{\text{nuc}})^{-5/6}. \quad (5)$$

The energy of the fluxtube state is at a minimum when the magnetic field H is $H_{c1} \lesssim H \lesssim H_{c2}$. For $H \lesssim H_{c1}$, the superconductor should be in a Meissner state (i.e., magnetic flux expulsion), while superconductivity is destroyed for $H \gtrsim H_{c2}$.

These conditions on κ and H (relative to H_{c1} and H_{c2}) determine in which regions in a NS are superconducting protons in a fluxtube or Meissner state. Figure 1 illustrates these cases for the APR nuclear EOS model and the CCDK model of the energy gap Δ (see below). We see that, for $H \lesssim 10^{15}$ G, a large portion of the NS interior would be in the Meissner (magnetic flux-free) state once superconductivity sets in. For $H \gtrsim 10^{15}$ G, the NS core retains its magnetic field, either in superconducting fluxtubes or in a non-superconducting state.

The above considerations were set out in [10] and explored since then. However, what has not been investigated quantitatively is whether magnetic flux expulsion by the

*Corresponding author: wynngo@slac.stanford.edu

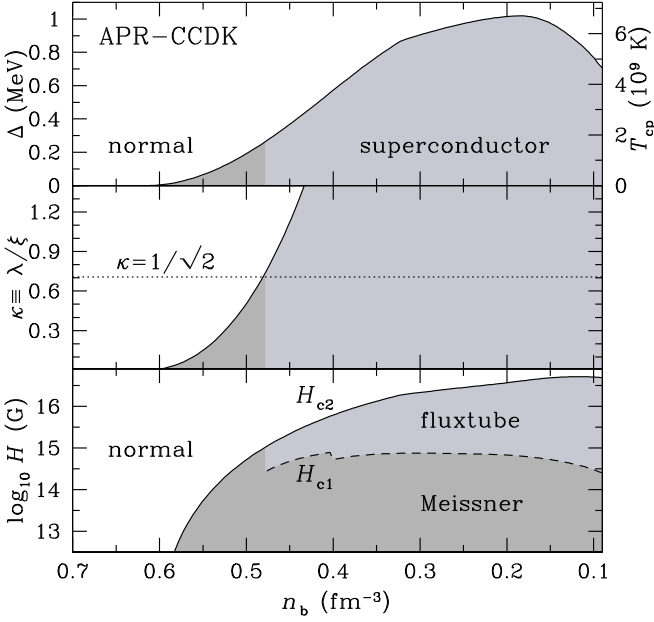


FIG. 1. Proton superconductor states. Top: CCDK model of singlet pairing energy gap Δ (left axis) and critical temperature T_{cp} (right axis) as a function of baryon number density n_b , calculated using the APR EOS model. Middle: Ratio κ between magnetic field penetration length scale λ and fluxtube size ξ . The two shaded regions separated at $n_b = 0.48 \text{ fm}^{-3}$ denote the regime where only the Meissner (flux expulsion) state is allowed (when $\kappa < 1/\sqrt{2}$) and the regime where the superconductor can be in Meissner state or in fluxtubes (when $\kappa > 1/\sqrt{2}$). Bottom: Dependence of superconductor state on n_b and magnetic field H . Superconductivity is destroyed when $H > H_{c2}$. The fluxtube state exists when $\kappa > 1/\sqrt{2}$ and $H_{c1} \lesssim H \lesssim H_{c2}$, and the Meissner state exists otherwise. The behavior of H_{c1} for $\kappa < 2$ is approximated using results from [9].

Meissner effect can occur fast enough as the NS cools soon after formation (as T drops below T_{cp}), although this issue is mentioned but not examined in past literature (see, e.g., [10,12,13]). In order for a Meissner state to be created, magnetic field must be expelled from the superconducting region (on the flux diffusion timescale) more rapidly than the region grows (on the cooling timescale). To find the former, [12] (see also [14] and Graber, in preparation) solves equations for flux diffusion and energy transfer at the fixed boundary between a superconducting region and a normal region. This calculation yields a (modified Ohmic) diffusion timescale (for $H/H_{c2} \ll 1$)¹

$$\begin{aligned} \tau_{\text{OhmH}} &\approx \tau_{\text{Ohm}} \frac{H}{2H_{c2}} = \frac{4\pi\sigma_c l_{\text{mag}}^2}{c^2} \frac{H}{2H_{c2}} \\ &= 4.4 \times 10^6 \text{ yr} \left(\frac{\sigma_c}{10^{29} \text{ s}^{-1}} \right) \left(\frac{l_{\text{mag}}}{1 \text{ km}} \right)^2 \left(\frac{H/2H_{c2}}{10^{-5}} \right), \end{aligned} \quad (6)$$

¹The calculation of τ_{OhmH} in [12] results in a scaling with respect to $H/2H_c$, where $H_c(T)$ is the thermodynamic critical field and usually satisfies $H_{c1} < H_c < H_{c2}$. For simplicity, we instead take the scaling to be $H/2H_{c2}$ since we are concerned with regimes where $H < H_{c2}$. Thus τ_{OhmH} given by Eq. (6) serves as a lower limit on the timescale.

where τ_{Ohm} is the magnetic field diffusion/dissipation timescale in non-superconducting matter, σ_c is electrical conductivity due to scattering, and l_{mag} is the length scale over which magnetic field changes. However, as we will show, cooling occurs much more rapidly than flux diffusion, such that τ_{OhmH} may not be the correct expulsion timescale. In superconducting matter, timescales are uncertain. Most estimates are many orders of magnitude longer than τ_{OhmH} [15–19], although [16,17] derive a superconducting induction equation with a magnetic field dissipation timescale

$$\tau_{\text{sc}} \approx 3.9 \times 10^7 \text{ yr} \left(\frac{n_{\text{nuc}}}{n_p} \right)^{1/6} \left(\frac{l_{\text{mag}}}{1 \text{ km}} \right)^2 \quad (7)$$

that can be shorter than τ_{OhmH} . Note that Eq. (7) uses a revised mutual friction drag [17]. While the processes that lead to Eqs. (6) and (7) may not be the exact description for flux expulsion from superconducting matter, τ_{OhmH} and τ_{sc} are the shortest known and possibly relevant timescales. Thus each serves as a useful limiting timescale, which is sufficient for our purposes. We also note the important role of l_{mag} , since at small enough values, both τ_{OhmH} and τ_{sc} can be very short.

In contrast, at ages $\lesssim 10^6$ yr, NSs cool via neutrino emission [20,21] over a timescale

$$\tau_{\text{cool}} = \frac{CT}{\epsilon_\nu} \sim 1 \text{ yr} \left(\frac{n_n}{n_e} \right)^{1/3} \left(\frac{10^9 \text{ K}}{T} \right)^6, \quad (8)$$

where $C = 1.6 \times 10^{20} \text{ erg cm}^{-3} \text{ K}^{-1} (n_n/n_{\text{nuc}})^{1/3} (T/10^9 \text{ K})$ is neutron heat capacity, $\epsilon_\nu \sim 3 \times 10^{22} \text{ erg cm}^{-3} \text{ s}^{-1} (n_e/n_{\text{nuc}})^{1/3} (T/10^9 \text{ K})^8$ is neutrino emissivity for modified Urca processes, and n_n is neutron density. The ratios of cooling to magnetic field diffusion timescales $\tau_{\text{cool}}/\tau_{\text{OhmH}}$ and $\tau_{\text{cool}}/\tau_{\text{sc}}$ are both $\sim 10^{-8}$ for $l_{\text{mag}} \approx 1 \text{ km}$. Clearly cooling occurs much more rapidly than flux expulsion until ages $\gtrsim 10^6$ yr when $T < 10^8 \text{ K}$. As a result, magnetic field cannot be expelled from macroscopic regions and is essentially frozen in nuclear matter. A NS core remains in a (metastable) magnetized state even though the minimum energy state is one with a flux-free configuration (see Fig. 1). In the following, we describe the NS models considered here, including the EOS and superconducting pairing gap, and present numerical results demonstrating quantitatively the estimates given above, as well as determine at what scale flux expulsion can occur. We note that [22] consider fluxtube motion from the NS core into the crust using the formulation of [16] that yields Eq. (7), whereas we consider superconductor formation/nucleation and Meissner flux expulsion within the core at the boundary $T_{cp}(n_b)$. Finally, we emphasize that, in order to test the maximum effectiveness of flux expulsion in comparison to cooling, we use a model which simulates slow NS cooling and ignore effects that would lead to more rapid cooling (see below).

II. NEUTRON STAR COOLING MODEL

To determine the evolution of the interior temperature of an isolated NS, we solve relativistic equations of energy balance and heat flux using the NS cooling code described in [23]. The initial temperature is taken to be a constant

$T e^\Phi = 10^{10}$ K, where Φ is the metric function corresponding to the gravitational potential in the Newtonian limit [24]. The envelope composition does not significantly affect cooling in the core, and thus we only consider an iron composition.

We consider three nuclear EOS models that produce a NS with maximum mass $M > 2 M_{\text{Sun}}$: APR, specifically A18+ δv + UIX* [25,26], and BSk20 and BSk21 [27–29]. NS models with $M > M_{\text{dU}}$ undergo the fast and efficient neutrino emission process known as direct Urca cooling (see, e.g., [20,21], for review), and $M_{\text{dU}} = 1.96 M_{\text{Sun}}$ for APR and $M_{\text{dU}} = 1.59 M_{\text{Sun}}$ for BSk21, while BSk20 does not produce NSs that undergo direct Urca cooling for any mass. As we will show, modified Urca cooling is fast enough to prevent flux expulsion. This would be even more so for NSs above the direct Urca threshold since direct Urca cooling operates on a much faster timescale. Thus we limit our study to $M < M_{\text{dU}}$.

For proton pairing gap, we consider three models, chosen because they span a range of densities and maximum energy gap: AO [30], BS [31], and CCDK [32], and we use the gap energy parametrization from [33]. Figure 1 shows the CCDK model of the energy gap $\Delta(n_b)$ using the APR EOS model. The CCDK model is one that has a large maximum energy gap and spans a broad density range. The AO model is one that has a small maximum energy gap and smaller density range but extends to high densities, while the BS model has a maximum energy gap intermediate between AO and CCDK but

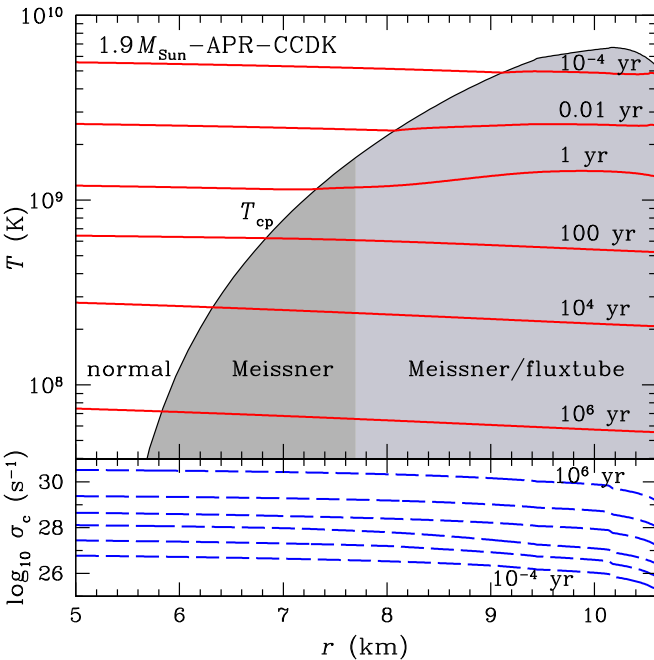


FIG. 2. Top: Temperature T as a function of radius r . The crust-core boundary is at $r \approx 10.7$ km, and total radius is 11.2 km for this $1.9 M_{\text{Sun}}$ NS built using the APR EOS. T_{cp} denotes the density-dependent critical temperature for onset of proton superconductivity (when $T < T_{\text{cp}}$) using the CCDK gap model. The separation between the two shaded regions is defined by $\kappa = 1/\sqrt{2}$ (see Fig. 1). Nearly horizontal curves show temperature profiles at various ages. Bottom: Radial profile of electrical conductivity σ_c at ages corresponding to temperature profiles shown in top panel.

is confined to relatively low densities (see [33]). For the CCDK proton gap model, the criterion $\kappa = 1/\sqrt{2}$ [see Eq. (1)] occurs at $n_b = 0.48 \text{ fm}^{-3}$ for the APR EOS model and at 0.69 fm^{-3} and 0.40 fm^{-3} for BSk20 and BSk21, respectively.

We do not consider superfluid neutrons in this work. The dominant effect of neutron superfluidity is to enhance cooling through neutrino emission from Cooper pairing [26,34]. Like the effect of direct Urca processes, this would lead to even shorter cooling times. It is possible that superfluid neutron-proton interactions could play a role (see, e.g., [35,36]), although this probably would not qualitatively change our conclusions.

III. RESULTS

A. High-mass NS with APR-CCDK models

To illustrate the primary findings of our work, we focus on results of one EOS model (APR) and one superconducting proton pairing gap model (CCDK). First we consider a high mass $1.9 M_{\text{Sun}}$ (11.2 km radius) NS, in order to probe higher densities than those of lower mass NSs. Since $M < M_{\text{dU}}$, only modified Urca and proton Cooper pairing processes operate in the core.

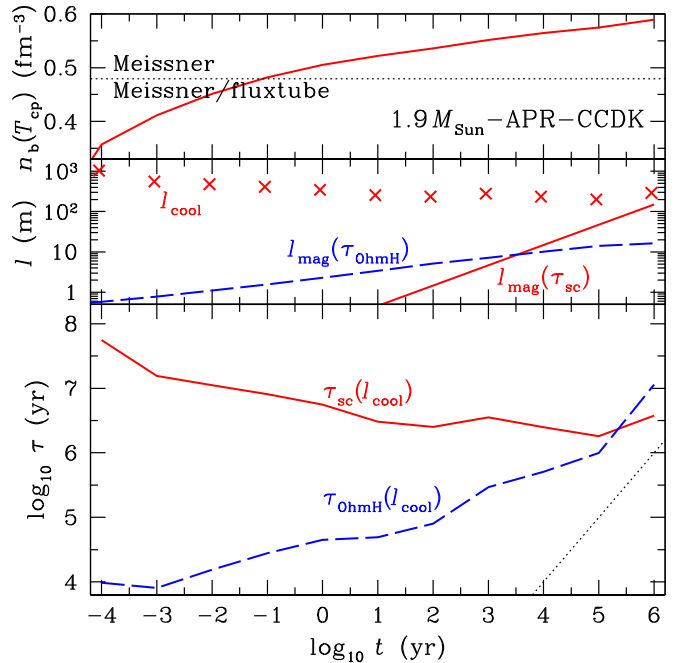


FIG. 3. Top: Density $n_b(T_{\text{cp}})$ at which onset of proton superconductivity occurs as a function of time t [since $T_{\text{cp}} = T(t)$]. Horizontal dotted line (at $n_b = 0.48 \text{ fm}^{-3}$, where $\kappa = 1/\sqrt{2}$) delineates regimes of Meissner and Meissner/fluxtube states (see Fig. 1). Middle: Crosses are radial distance over which the superconducting region grows at each cooling epoch and we define as cooling length scale l_{cool} . Dashed line is the length scale l_{mag} obtained using Eq. (6) and setting $\tau_{\text{OhmH}} = t$, while the solid line corresponds to using Eq. (7) and setting $\tau_{\text{sc}} = t$. Bottom: Flux diffusion timescales τ_{OhmH} and τ_{sc} with $l_{\text{mag}} = l_{\text{cool}}$, where l_{cool} is from the middle panel. Dotted line is $\tau = t$. In middle and bottom panels, $H/2H_{c2} = 10^{-5}$ is assumed.

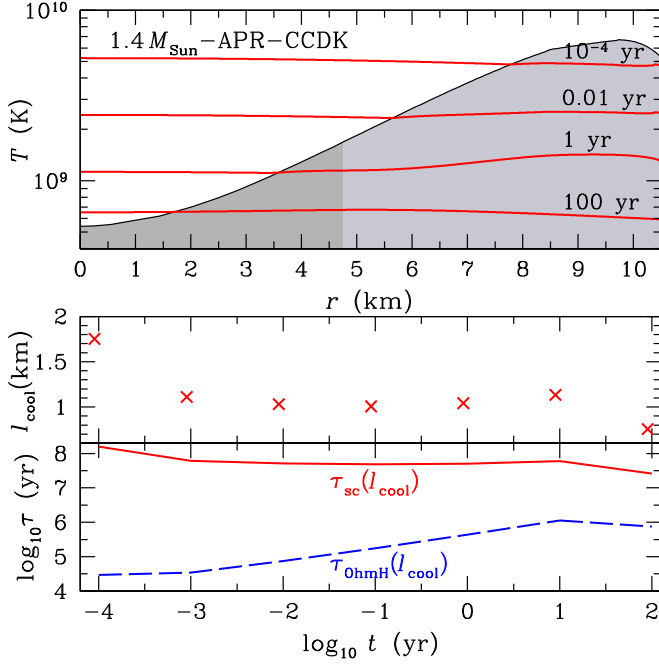


FIG. 4. Top: Temperature T as a function of radius r . The crust-core boundary is at $r \approx 10.6$ km, and total radius is 11.6 km for this $1.4 M_{\text{Sun}}$ NS built using the APR EOS. The separation between the two shaded regions is defined by $\kappa = 1/\sqrt{2}$ (see Fig. 1). Nearly horizontal curves show temperature profiles at various ages. Middle: Crosses are radial distance over which the superconducting region grows at each cooling epoch and we define as cooling length scale l_{cool} . Dashed line is the length scale l_{mag} obtained using Eq. (6) and setting $\tau_{\text{OhmH}} = t$, while the solid line corresponds to using Eq. (7) and setting $\tau_{\text{sc}} = t$. Bottom: Flux diffusion timescales τ_{OhmH} and τ_{sc} with $l_{\text{mag}} = l_{\text{cool}}$, where l_{cool} is from the middle panel. In middle and bottom panels, $H/2H_{c2} = 10^{-5}$ is assumed.

Figure 2 shows the evolution of the core temperature profile from our cooling simulation using the APR EOS and CCDK pairing gap models. When a NS is only several minutes old, the temperature drops below the maximum critical temperature [$T < T_{\text{cp}}(0.2 \text{ fm}^{-3})$]; see Fig. 1, such that a proton superconductor begins to form at $r \sim 10$ km. At subsequent times, the superconducting region grows and encompasses more of the star.

The top panel of Fig. 3 shows the superconducting boundary [at $n_{\text{b}}(T_{\text{cp}})$; see Fig. 1] as a function of time, while the middle panel shows the increase in radial extent of the superconducting region l_{cool} as the NS cools. The latter is calculated at each logarithmic decade in time ($\log t_i = i$, where $i = -4, -3, \dots, 6$) and $l_{\text{cool}} = r[T_{\text{cp}}(t_i)] - r[T_{\text{cp}}(t_{i-1})]$. We see that the superconducting region grows by hundreds of meters every $\Delta \log t = 1$ due to cooling of the NS. Note that we could consider shorter time intervals, so that the cooling length scale is smaller, but this would necessarily imply shorter cooling timescales as well.

In order for magnetic flux to be expelled from a Meissner region, diffusion of magnetic field must occur over a length scale l_{mag} which is greater than the cooling length scale l_{cool} ; otherwise magnetic flux is unable to vacate an ever-increasing superconducting region. We can obtain a minimum flux expulsion timescale τ_{OhmH} by computing the electrical conductivity σ_{c} ([37]; see bottom panel of Fig. 2) and

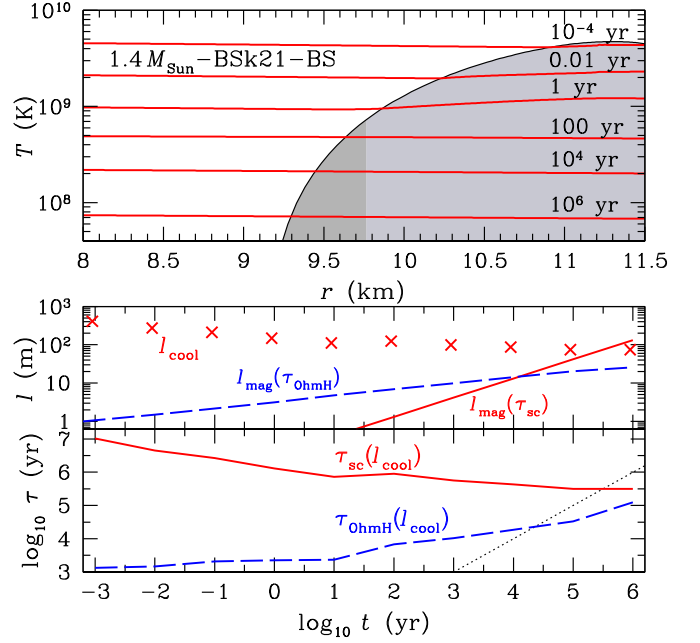


FIG. 5. Top: Temperature T as a function of radius r . The crust-core boundary is at $r \approx 11.5$ km, and total radius is 12.6 km for this $1.4 M_{\text{Sun}}$ NS built using the BSk21 EOS. The separation between the two shaded regions is defined by $\kappa = 1/\sqrt{2}$ (see Fig. 1). Nearly horizontal curves show temperature profiles at various ages. Middle: Crosses are radial distance over which the superconducting region grows at each cooling epoch and we define as cooling length scale l_{cool} . Dashed line is the length scale l_{mag} obtained using Eq. (6) and setting $\tau_{\text{OhmH}} = t$, while the solid line corresponds to using Eq. (7) and setting $\tau_{\text{sc}} = t$. Bottom: Flux diffusion timescales τ_{OhmH} and τ_{sc} with $l_{\text{mag}} = l_{\text{cool}}$, where l_{cool} is from the middle panel. Dotted line is $\tau = t$. In middle and bottom panels, $H/2H_{c2} = 10^{-5}$ is assumed.

conservatively setting $H/2H_{c2} = 10^{-5}$ (e.g., $10^{11} \text{ G}/10^{16} \text{ G}$) and $l_{\text{mag}} = l_{\text{cool}}$ in Eq. (6). Alternatively, if we consider τ_{sc} as the flux expulsion timescale, we find a minimum timescale by setting $l_{\text{mag}} = l_{\text{cool}}$ in Eq. (7). The bottom panel of Fig. 3 shows these timescales $\tau_{\text{OhmH}}(l_{\text{cool}})$ and $\tau_{\text{sc}}(l_{\text{cool}})$ as functions of time t . It is clear that $t \ll \tau_{\text{OhmH}}, \tau_{\text{sc}}$ at every epoch, i.e., the NS cools at a much faster rate than the rate at which magnetic flux can be expelled from superconducting regions. Therefore magnetic field is retained within the NS core until at least 10^6 yr.

We estimate the growing size of flux-free nucleation regions by setting $\tau_{\text{OhmH}} = t$ in Eq. (6) or $\tau_{\text{sc}} = t$ in Eq. (7) and solving for $l_{\text{mag}}(t)$. Results are shown in the middle panel of Fig. 3. Flux expulsion creates Meissner state regions of size ~ 10 m (for $H/2H_{c2} = 10^{-5}$) or ~ 100 m after 10^6 yr, depending on whether expulsion occurs on the timescale of τ_{OhmH} or τ_{sc} , respectively. In addition, instead of comparing timescales, the fact that $l_{\text{cool}} \gg l_{\text{mag}}$ when $t < 10^6$ yr indicates the superconducting region expands by a much larger distance than the distance over which magnetic field is expelled.

B. Intermediate-mass NS with APR-CCDK models

Figure 4 shows results for a lower mass ($1.4 M_{\text{Sun}}$) NS. The central density for this NS is $n_{\text{b}} \approx 0.56 \text{ fm}^{-3}$, which is near the boundary defined by $\kappa = 1/\sqrt{2}$ at 0.48 fm^{-3} . The top

panel illustrates the fact that nearly the entire core could be in the Meissner state if magnetic flux is expelled once $T < T_{cp}$ (at $t >$ a few hundred years). However, the middle and bottom panels show a cooling length scale $l_{cool} \sim 1$ km (larger than for a $1.9 M_{Sun}$ NS) and flux diffusion timescales $\tau_{OhmH}, \tau_{sc} \gg t$, respectively. Therefore magnetic flux can be expelled from the entire core only after at least 10^7 yr.

C. Other EOS and proton superconducting gaps

We perform analogous calculations as those described above but using different combinations of the APR, BSk20, or BSk21 nuclear EOS model and the AO, BS, or CCDK proton pairing gap model. The results using the CCDK model and either BSk20 or BSk21 are qualitatively similar to those using APR. The AO gap model is fairly broad and extends to higher densities than BS. Results using this model are similar to those of CCDK, except times/ages at which transitions occur later due to the lower overall Δ (and T_{cp}). The BS gap model is relatively narrow and centered at low densities; for all three EOS models, the superconducting region is near the crust-core boundary and has a radial width $\lesssim 2$ km. Figure 5 shows results for a $1.4 M_{Sun}$ NS built using the BSk21 EOS model. Flux expulsion from this narrow superconducting region could occur in $\sim 10^4$ yr for relatively low ($\sim 10^{10}$ G) magnetic fields.

IV. CONCLUSIONS

In summary, we performed detailed cooling simulations to study the onset of proton superconductivity in NS cores and

confirmed previous estimates that the core retains its magnetic field even though the minimum energy state is one in which magnetic flux is expelled due to the Meissner effect. This is because a dynamical NS cools so rapidly (even under the assumption of slow cooling) that the superconducting region expands much faster than the field can be expelled by any known processes. To produce a large region in the core devoid of magnetic field, the field must diffuse over macroscopic scales of order a kilometer or more, and the timescale for such field diffusion is $\gtrsim 10^7$ yr. At 10^6 yr, the size of flux-free regions is probably < 10 m and at most ~ 100 m (see middle panels of Figs. 3 and 5). This suggests that there is not significant magnetic field evolution in the core of NSs younger than at least 10^7 yr [see Eq. (6) or (7); see also [22]]. Our results apply to NSs with $H > 10^{11}$ G, including magnetars, most of which have $H \gtrsim 10^{14}$ G. Thus for observed magnetars with age $< 10^5$ yr, there is a limit to the amount of field decay that can occur if the magnetic field in the crust is anchored in the core.

ACKNOWLEDGMENTS

W.C.G.H. is grateful to K. Glampedakis, A. Schmitt, and A. Sedrakian for discussions. W.C.G.H. appreciates use of computer facilities at KIPAC. W.C.G.H. and N.A. acknowledge support through grant no. ST/M000931/1 from Science and Technology Facilities Council (STFC) in the UK. V.G. is supported by a McGill Space Institute post-doctoral fellowship and Trottier Chair in Astrophysics and Cosmology.

-
- [1] P. Haensel, A. Y. Potekhin, and D. G. Yakovlev, *Neutron Stars I. Equation of State and Structure* (Springer, New York, 2007).
 - [2] J. M. Lattimer and M. Prakash, *Phys. Rep.* **621**, 127 (2016).
 - [3] D. Page, M. Prakash, J. M. Lattimer, and A. W. Steiner, *Phys. Rev. Lett.* **106**, 081101 (2011).
 - [4] P. S. Shternin, D. G. Yakovlev, C. O. Heinke, W. C. G. Ho, and D. J. Patnaude, *Mon. Not. R. Astron. Soc.* **412**, L108 (2011).
 - [5] K. G. Elshamouty, C. O. Heinke, G. R. Sivakoff, W. C. G. Ho, P. S. Shternin, D. G. Yakovlev, D. J. Patnaude, and L. David, *Astrophys. J.* **777**, 22 (2013).
 - [6] B. Posselt, G. G. Pavlov, V. Suleimanov, and O. Kargaltsev, *Astrophys. J.* **779**, 186 (2013).
 - [7] J. A. Sauls, in *Timing Neutron Stars*, edited by H. Ögelman and E. P. J. van den Heuvel (Kluwer Academic, New York, 1989), p. 457.
 - [8] D. Page, J. M. Lattimer, M. Prakash, and A. W. Steiner, in *Novel Superfluids*, edited by K. H. Bennemann and J. B. Ketterson (Oxford University Press, Oxford, 2014), Vol. 2, p. 505.
 - [9] M. Tinkham, *Introduction to Superconductivity*, 2nd ed. (McGraw-Hill, Inc., New York, 1996).
 - [10] G. Baym, C. Pethick, and D. Pines, *Nature* **224**, 673 (1969).
 - [11] V. Graber, N. Andersson, and M. Hogg, *Int. J. Mod. Phys. D* **26**, 1730015 (2017).
 - [12] G. Baym, *Neutron Stars* (Nordita, Copenhagen, 1970).
 - [13] M. Sinha and A. Sedrakian, *Phys. Part. Nucl.* **46**, 826 (2015).
 - [14] A. B. Pippard, *The London, Edinburgh, and Dublin Phil. Mag. J. Sci.* **41**, 243 (1950).
 - [15] K. Glampedakis, D. I. Jones, and L. Samuelsson, *Mon. Not. R. Astron. Soc.* **413**, 2021 (2011).
 - [16] V. Graber, N. Andersson, K. Glampedakis, and S. K. Lander, *Mon. Not. R. Astron. Soc.* **453**, 671 (2015).
 - [17] V. Graber, Ph.D. thesis, University of Southampton (2016).
 - [18] V. A. Dommes and M. E. Gusakov, *Mon. Not. R. Astron. Soc. Lett.* **467**, L115 (2017).
 - [19] A. Passamonti, T. Akgün, J. A. Pons, and J. A. Miralles, *Mon. Not. R. Astron. Soc.* **469**, 4979 (2017).
 - [20] D. G. Yakovlev and C. J. Pethick, *Annu. Rev. Astron. Astrophys.* **42**, 169 (2004).
 - [21] A. Y. Potekhin, J. A. Pons, and D. Page, *Space Sci. Rev.* **191**, 239 (2015).
 - [22] J. G. Elfritz, J. A. Pons, N. Rea, K. Glampedakis, and D. Viganò, *Mon. Not. R. Astron. Soc.* **456**, 4461 (2016).
 - [23] W. C. G. Ho, K. Glampedakis, and N. Andersson, *Mon. Not. R. Astron. Soc.* **422**, 2632 (2012); **425**(E), 1600 (2012).
 - [24] S. L. Shapiro and S. A. Teukolsky, *Black Holes, White Dwarfs, and Neutron Stars* (John Wiley and Sons, New York, 1983).
 - [25] A. Akmal, V. R. Pandharipande, and D. G. Ravenhall, *Phys. Rev. C* **58**, 1804 (1998).
 - [26] D. Page, J. M. Lattimer, M. Prakash, and A. W. Steiner, *Astrophys. J. Suppl.* **155**, 623 (2004).

- [27] N. Chamel, S. Goriely, and J. M. Pearson, [Phys. Rev. C **80**, 065804 \(2009\)](#).
- [28] S. Goriely, N. Chamel, and J. M. Pearson, [Phys. Rev. C **82**, 035804 \(2010\)](#).
- [29] A. Y. Potekhin, A. F. Fantina, N. Chamel, J. M. Pearson, and S. Goriely, [Astron. Astrophys. **560**, A48 \(2013\)](#).
- [30] L. Amundsen and E. Østgaard, [Nucl. Phys. A **437**, 487 \(1985\)](#).
- [31] M. Baldo and H.-J. Schulze, [Phys. Rev. C **75**, 025802 \(2007\)](#).
- [32] J. M. C. Chen, J. W. Clark, R. D. Davé, and V. V. Khodel, [Nucl. Phys. A **555**, 59 \(1993\)](#).
- [33] W. C. G. Ho, K. G. Elshamouty, C. O. Heinke, and A. Y. Potekhin, [Phys. Rev. C **91**, 015806 \(2015\)](#).
- [34] M. E. Gusakov, A. D. Kaminker, D. G. Yakovlev, and O. Y. Gnedin, [Astron. Astrophys. **423**, 1063 \(2004\)](#).
- [35] M. G. Alford and G. Good, [Phys. Rev. B **78**, 024510 \(2008\)](#).
- [36] A. Haber and A. Schmitt, [Phys. Rev. D **95**, 116016 \(2017\)](#).
- [37] G. Baym, C. Pethick, and D. Pines, [Nature **224**, 674 \(1969\)](#).